2020 IEEE International Conference on Robotics and Automation (ICRA)
31 May - 31 August, 2020. Paris, France

Flow Compensation for Hydraulic Direct-Drive System with a Single-rod Cylinder Applied to Biped Humanoid Robot

J. Shimizu, T. Otani, H. Mizukami, K. Hashimoto, and A. Takanishi, *Member, IEEE*

Abstract— **Biped robots require massive power on each leg while walking, hopping, and running. We have developed a flow-based control system—called hydraulic direct drive system—that can achieve high output while avoiding spatial limitations. To implement the proposed system with simple equipment configuration, a pump and single-rod cylinder are connected in a closed loop. However, because compensation for flow rate is impossible in a completely closed loop, owing to the difference in the pressure receiving area caused by the rod, a passive flow compensation valve is employed. This valve has a simple structure and is easy to implement. Further, an additional sensor is required to detect the open/close state because the valve state will cause an error in flow control. Therefore, we implemented a model in the controller to predict the state of the flow compensation valve and formulated a method of switching from flow control to pressure control according to the predicted state. Experimental results indicate that the error of the joint angle is reduced to less than 1.6 degrees for walking patterns, and stable walking is realized when the system is installed in biped humanoid robots.**

I. Introduction

Methodical approaches are required to safely and quantitatively evaluate products such as shoes, walking aids, and canes. One such approach is based on user evaluations, which may lead to safety risks and reproducibility problems. We previously proposed an effective approach for performing these evaluations with a biped humanoid robot. A robot, named WABIAN-2R (WAseda BIpedal humANoid - No. 2 Refined), was fitted with a pelvis model and exhibited a stretched knee gait [1]. To expand the scope of evaluation, the athletic performance should be improved to realize not only walking but also hopping and running. High-power actuators are required for such a robot. However, because such high-power electric motors are large, the installation of such motors in human-sized robots is difficult owing to space limitations. To resolve this problem, we proposed a mechanical system that enables the production of large torque with pelvic oscillation and leg elasticity [2].

To increase the output of electrical motors, Urata et al. developed a technique that improves the continuous output torque using a liquid cooling system [3]. Other researchers have proposed mounting two motors on the driving axes of robots [4, 5]. These approaches have provided high-speed and -torque joints in both legs of the humanoids. Further, although this system improves the output of each axis, high output is not obtained at all joints automatically during walking, running, and hopping. Therefore, it is effective to share the output of the drive source for driving each joint.

There are robots that have realized dynamic operation by utilizing the hydraulic system that can share the outputs of the driving sources. Examples of these are Boston Dynamics's ATLAS [6] for biped humanoid robots and Khan's MiniHyQ [8] for quadruped robots. There is also Hyon's TeaMu that reproduces link length and weight ratio of a human by utilizing the excellent layout of the hydraulic system. These robots use proportional valves to control the power supplied to each axis from a pressure source. However, the control system based on proportional valves leads to reduced energy efficiency because of pressure loss in the valves.

A displacement control system that controls the actuator speed with the pump derived flow has been recommended to reduce the hydraulic energy loss in valves [9, 10]. An example of the displacement control to a robot system is Kaminaga's electro-hydrostatic actuator (EHA) [11]. The proposed EHA is based on closed circuit and uses a through-rod cylinder suitable for closed circuit. Such a cylinder is difficult to mount and has lower thrust than a single-rod cylinder. Hyon et al. proposed a hydraulic hybrid servo booster to extend the capability of the EHA [12,13]. Although this system can simultaneously achieve high output and accuracy with a single-rod cylinder, two types of pumps and four valves are required for the cylinder. However, such an increase in equipment is undesirable for biped humanoid robots that host their actuation system onboard.

We previously proposed a hydraulic direct-drive system based on a flow-based control system employing a pump that uses a single-rod cylinder, which can be used for biped humanoid robots [14]. The hydraulic direct-drive system achieved excellent energy savings and nearly perfect position tracking at the steady state [14]. The proposed hydraulic

*This study was conducted with the support of the Research Institute for Science and Engineering, Waseda University; Future Robotics Organization, Waseda University, and as a part of the humanoid project at the Humanoid Robotics Institute, Waseda University. We would like to thank Editage (www.editage.jp) for English language editing.

J. Shimizu is with the Graduate School of Advanced Science and Engineering, Waseda University, and is also a researcher at Hitachi, Ltd., #41-304, 17 Kikui-cho, Shinjuku-ku, Tokyo 162-0044, JAPAN (e-mail: contact@takanishi.mech.waseda.ac.jp).

T. Otani is with the Department of Modern Mechanical Engineering, Waseda University; and is is also a researcher at the Humanoid Robotics Institute (HRI), Waseda University.

H. Mizukami is with the Graduate School of Creative Science and Engineering, Waseda University.

K. Hashimoto is with the School of Science and Technology, Meiji University; and is also a researcher at the Humanoid Robotics Institute, Waseda University.

A. Takanishi is with the Department of Modern Mechanical Engineering, Waseda University; and is the director of the Humanoid Robotics Institute, Waseda University.

direct-drive system can hydraulically connect multiple systems. Therefore, by sharing the output of the pump for each leg, the load on the motor that drives each pump can be reduced along with the motor size. The result of the hopping simulation exhibited a 35.6% reduction in motor output [15]. In addition, we proposed a hydraulic interlocking drive system considering the cyclic and symmetrical motions of biped robots such as walking and running. The hydraulic interlocking drive system achieved a 27.3% reduction in the motor power of the hip pitch joint for walking patterns [16].

Previous studies have adopted a closed loop connection between a pump and a single rod cylinder as a simple device configuration when implementing a hydraulic direct-drive system. In the closed circuit, a passive flow compensation valve was implemented to compensate for the flow error due to the difference in the pressure receiving area caused by the single-rod cylinder. However, because the control does not consider the state of the passive flow compensation valve, the error increases when the cylinder drive direction changes.

This paper proposes a control system that predicts the state of the passive flow compensation valve. As the valve cannot directly measure the internal state, the proposed system uses a state prediction model to determine the state. If the port of the passive flow compensation valve connected to the pump discharge side is predicted to be open, the system switches to the pressure control mode based on the demand pump discharge pressure to rapidly shift to the closed state. The demand pressure is calculated based on the demand flow rate to the cylinder and the opening area of the proportional valve on the discharge side. Satisfactory trajectory tracking performance is achieved by controlling the passive flow control valve at an appropriate state. A performance comparison with the case where this system is not applied demonstrated the feasibility of the proposed system.

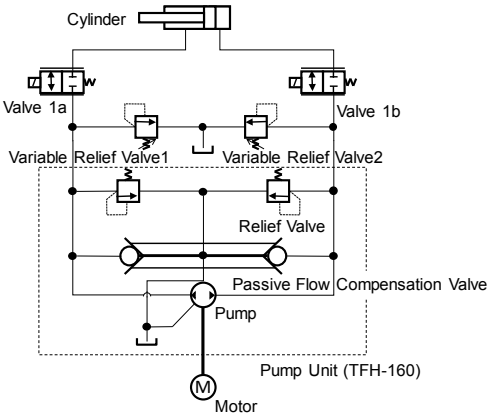

Figure 1. Hydraulic direct-drive circuit

TABLE I. HYDRAULIC CIRCUIT PARAMETERS

Pump Displacement (cc/rev)		1.6
Pump relief pressure (MPa)		21
Cylinder stroke (mm)		132
Cylinder piston diameter (mm)		25
Cylinder rod diameter (mm)		16
Variable Relief Valve Set Pressure (MPa)		4.
Variable Relief Valve Override (MPa/(L/min))		1/8.0
Hose Inner Diameter (mm)		6.4
Hose Length (mm)	**Pump to Valves 1a, 1b**	300
	Valves 1a, 1b to Cylinder	1000
Valves 1a, 1b Nominal Flow Rate (L/min/(MPa))		5/1
Oil Kinematic Viscosity (mm^2/s)	**40 (°C)**	14.68
	100 (°C)	3.717
Experimental Oil Temperature (°C)		25

The remainder of this paper is organized as follows. Section II introduces the design of the flow compensation system and its theoretical model. Section III presents the experimental set-up, procedure, and results. Finally, Section IV presents concluding remarks and the directions for future work.

II. FLOW COMPENSATION SYSTEM

A. Description

We developed the hydraulic circuit shown in Fig. 1 to implement the proposed hydraulic direct-drive system [14]. In the figure, the pump unit and cylinder are connected through Valves 1a and 1b. A pump unit [17] manufactured by Takako Industries is incorporated into the system. The pump unit includes a pump, relief valves to protect the pump, and a special check valve unit. The pump has two ports and flow can output from both ports. The passive flow compensation valve has two check valves, which are interconnected by a rod. Therefore, this unit connects the lower pressure side of the pump outlet to the tank. Valves 1a and 1b are solenoid proportional valves. The circuit has two variable relief valves that can tune the relief pressure. The hydraulic parameters are listed in Table I.

By directly connecting the cylinder and pump in a closed circuit as shown in Fig. 1, the speed and direction of the cylinder can be controlled directly by the pump. Furthermore, as the motor is more responsive than the general directional control valve, a system with high responsiveness can be constructed by directly controlling the rotation direction of the pump with a motor. In addition, a higher response characteristic can be obtained by controlling the flow rate with a motor, as shown in Fig. 1, rather than with a proportional valve [14].

When the single-rod cylinder and the pump are connected in a closed circuit, the error between the cylinder inflow and outflow due to the difference in the pressure receiving area becomes a problem. The pump discharge flow rate, $Q_{pump\ out}$, is equal to the meter-in flow to the cylinder, $Q_{cyl\ in}$.

$$Q_{cyl\ in} = Q_{pump\ out}. \tag{1}$$

At this time, the meter-out flow $Q_{cyl\ out}$ is

$$Q_{cyl\ out} = \alpha\, Q_{cyl\ in}, \tag{2}$$

where α is the pressure receiving area ratio.

$$\alpha = \begin{cases} \frac{A_{CylRod}}{A_{CylCap}} & (V_{dCyl} > 0 : Outstroke) \\ \frac{A_{CylCap}}{A_{CylRod}} & (V_{dCyl} < 0 : Instroke) \end{cases}. \tag{3}$$

Although the pump discharge flow rate $Q_{pump\ out}$ is equal to the suction flow rate $Q_{pump\ in}$, the return flow rate from the cylinder $Q_{cyl\ out}$ is greater than the pump discharge flow rate $Q_{pump\ out}$ in the cylinder instroke motion, and the cylinder return flow rate $Q_{cyl\ out}$ is less than the pump discharge flow

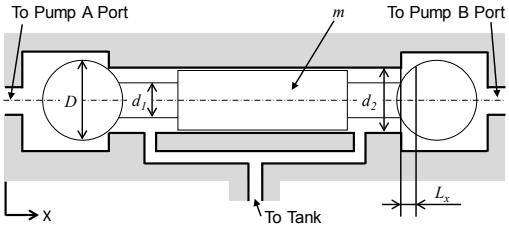

Figure 2. Model of passive flow compensation valve

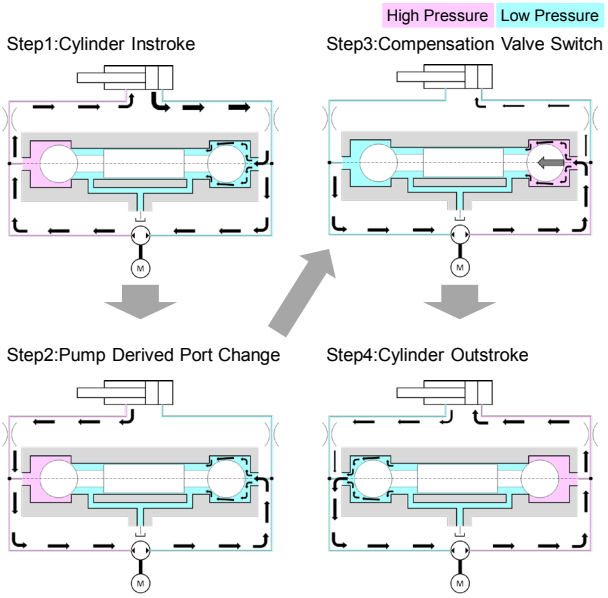

Figure 3. State of the passive flow compensation valve

rate $Q_{pump\ out}$ in the outstroke. Therefore, it is necessary to flush the excess flow rate outside the closed circuit. When extending the cylinder, the pump discharge flow rate is equal to the flow rate on the cap side, and the flow rate returning from the rod side is insufficient. Therefore, it is necessary to compensation for the insufficient flow rate from outside the closed circuit.

The passive flow compensation valve connects the tank to the low-pressure side. In the proposed hydraulic direct drive system shown in Fig. 1, the discharge flow rate of the single rod cylinder is controlled using a proportional valve. Therefore, in the steady state, the pressure on the suction side of the pump is lower than that on the discharge side; hence, the passive flow compensation valve is connected to the tank at the suction side of the pump. This makes it possible to flush excess flow and charge insufficient flow.

The passive flow compensation valve achieves the abovementioned characteristics in the steady state; however, in the transient region immediately after the pump discharge switch, the pump discharge side and tank are connected. The pump discharge flow rate and cylinder inflow rate do not match, causing an error with respect to the target speed of the cylinder.

B. Model

The passive flow compensation valve has ports for pump A, pump B, and the tank. The port with the lower pressure (port A or port B) is connected to the tank. The passive flow compensation valve is described as a structure in which two check valves are connected by a rod; however, the detailed structure and internal dimensions are not disclosed.

Based on the structure of a general check valve, the passive flow compensation valve is modeled as shown in Fig. 2. The modeled valve has a poppet that connects the two balls (diameter D) with a rod (diameter d_1). L_x is the stroke of the poppet. Furthermore, the poppet seal diameter is d_2.

The steady axial force F_s acting on the poppet is

$$F_s = (\mathrm{P}_{pump\ out} - \mathrm{P}_{pump\ in})\left(\frac{D}{2}\right)^2 \pi - \rho Q_{pump\ out} u_1, \quad (4)$$

where u_1 is the flow velocity, ρ is the density of the fluid, and $Q_{pump\ out}$ is pump derived flow rate. The first term in (4) represents the force generated when the pressure hits the pressure receiving surface of the poppet. The second term represents the force generated by the fluid force. In this prediction model, the second term is neglected because the flow rate immediately after switching is low. The equation of motion for the poppet valve is

$$m\frac{d^2x}{dt^2} + B_f\frac{dx}{dt} = F_s + f_{s0}\,, \quad (5)$$

where B_f is the viscous friction coefficient and f_{s0} is the static maximum friction coefficient. Using (1) and (2), the equation of motion of the poppet can be expressed as follows:

$$\frac{d^2x}{dt^2} + \frac{B_f}{m}\frac{dx}{dt} - \frac{(\mathrm{P}_{pump\ out} - \mathrm{P}_{pump\ in})\left(\frac{D}{2}\right)^2\pi}{m} - \frac{f_{s0}}{m} = 0\,. \quad (6)$$

Using (6), the internal state of the passive flow compensation valve can be estimated.

Fig. 3 shows the behavior of the passive flow compensation valve model when switching from instroke to outstroke.

Step 1: During cylinder instroke, the pump discharge flow $Q_{pump\ out}$ is supplied to the cylinder rod. The cylinder meter-out flow rate from the cap side is larger than the pump suction flow rate $Q_{pump\ in}$. The passive flow compensation valve connects port B of the pump and tank because the pressure of port A on the discharge side of the pump is higher than that of port B on the suction side. Therefore, the surplus portion of the cylinder meter-out flow is discharged to the tank via the passive flow compensation valve.

Step 2: Immediately after switching to the cylinder outstroke, the pump suction pressure is higher than the pump discharge pressure, and the passive flow compensation valve is connected to port B and the tank. Therefore, the pump discharge flow is discharged to the tank.

Step 3: As the pump discharge flow rate increases, the pump discharge pressure increases and the force that drives the poppet is generated. Part of the pump discharge flows into the cylinder.

Step 4: When the poppet is completely closed between port B and the tank, all the pump discharge flow is supplied to the cylinder.

In Steps 2 and 3, the cylinder velocity cannot directly be controlled by the pump discharge flow rate. This leads to an

error when the driving direction of the cylinder is switched [14]. In this transient state, to control the supply to the cylinder based on the pump discharge flow rate, the passage flow rate of the passive flow compensation valve, which is a disturbance, is required. As the flow rate of a small passive flow compensation valve is difficult to directly measure, it must be predicted. However, because the opening area of the passive flow compensation valve is not constant, predicting the flow rate through the passive flow compensation valve is not straightforward.

When the opening area A_{PV} of proportional Valves 1a and 1b is constant, the flow rate to the cylinder through the proportional valve is determined by the pump discharge pressure $P_{pump\ out}$ and the cylinder cap pressure $P_{cyl\ cap}$:

$$Q_{cyl\ in} = A_{PV} C_d \sqrt{\frac{2\,(P_{pump\ out} - P_{cyl\ meter\ in})}{\rho}}. \tag{7}$$

where C_d is the flow coefficient. In this study, petroleum fluid was used as the fluid for the experiment. Fluctuation in hydraulic pressure ΔP in a fixed volume chamber is

$$\Delta P = \Delta V \frac{K}{V_0}. \tag{8}$$

where V_0 is the initial volume of the container, K is the bulk modulus, and ΔV is the volume of the hydraulic fluid flowing into the chamber. The temporal change in the inflow volume ($\Delta V/\Delta t$) is defined as the flow rate Q. Based on (8), the temporal change in pressure can be controlled by the flow rate into the chamber.

$$\frac{\Delta P}{\Delta t} = \frac{\Delta V}{\Delta t}\frac{K}{V_0},$$
$$\frac{dP}{dt} = Q\frac{K}{V_0}. \tag{9}$$

From (7), the demand pump discharge pressure $P_{pump\ out\ d}$ to the demand meter-in flow rate of the cylinder $Q_{cyl\ in\ d}$ is

$$P_{pump\ out\ d} = \frac{\rho}{2}\left(\frac{Q_{cyl\ in\ d}}{A_{PV} C_d}\right)^2 + P_{cyl\ meter\ in}. \tag{10}$$

The demand pump discharge flow rate $Q_{pump\ out\ d}$ is expressed using (9) and (10)

$$Q_{pump\ out\ d} = \frac{V_0}{K}\frac{(P_{pump\ out\ d} - P_{pump\ out\ act})}{dt},$$
$$= \frac{V_0}{K}\frac{\left(\frac{\rho}{2}\left(\frac{Q_{cyl\ in\ d}}{A_{PV} C_d}\right)^2 + P_{cyl\ meter\ in} - P_{pump\ out\ act}\right)}{dt}. \tag{11}$$

$P_{pump\ out\ act}$ is the actual pump discharge pressure. $Q_{cyl\ in\ d}$ can be controlled even in the transient region by controlling the pump discharge pressure $P_{pump\ out\ act}$ that can be measured.

The block diagram of the pressure-based control in the proposed system is shown in Fig. 4. As shown in this figure, the demand cylinder meter-in flow rate $Q_{d\ Cyl\ in}$ based on the demand joint angle θ_d, is the same as the previously proposed flow rate control [14]. The demand pump discharge pressure $P_{pump\ out\ d}$ is calculated from the demand cylinder meter-in flow rate $Q_{d\ Cyl\ in}$, cylinder meter-in pressure $P_{cyl\ meter\ in}$, and the fixed opening area $A_{d\ Valve\ const}$ of the proportional valve. Based on the difference between the pump demand

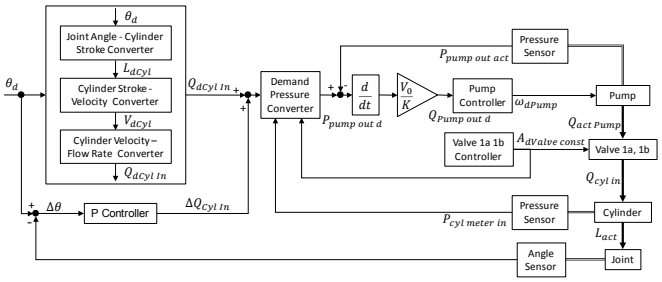

Figure 4. Block diagram of pressure-based control mode

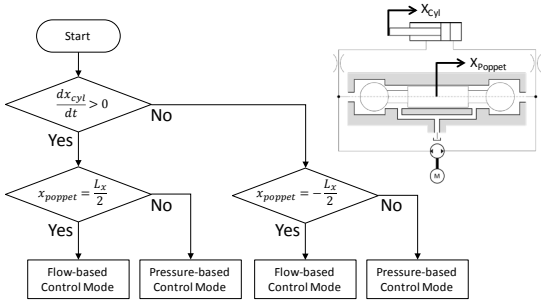

Figure 5. Control mode select flow

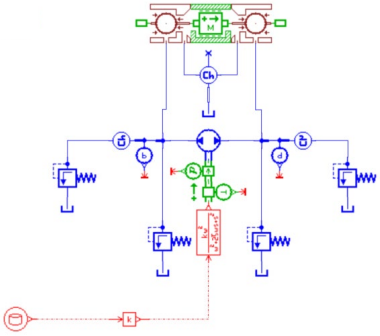

Figure 6. Simulation model

discharge pressure $P_{pump\ out\ d}$ and the actual pressure $P_{pump\ out\ act}$, the demand pump discharge flow $Q_{pump\ out\ d}$ rate is calculated by (11).

In the steady state, flow-based control is performed as in the previous report [14], and pressure control is performed in the transient state. The control mode is selected based on the required cylinder speed and the position of the poppet of the passive flow compensation valve (Fig. 5). Therefore, knowledge of the internal state of the passive flow compensation valve is required to determine whether it is steady or transient. It is difficult to directly measure the state of a passive flow compensation valve owing to size constraints. Therefore, we built a model that predicts the internal state.

The internal structure of the passive flow compensation valve has not been disclosed. Therefore, a state prediction model for the passive flow compensation valve was constructed from the measurements. The unknown parameters from the measurements in the equation of motion of the valve is validated in (6).

The poppet inside the valve was modeled based on (6); however, the other hydraulic behavior was modeled using a physical modeling tool, LMS Imagine.Lab Amesim™ (Siemens K.K.).

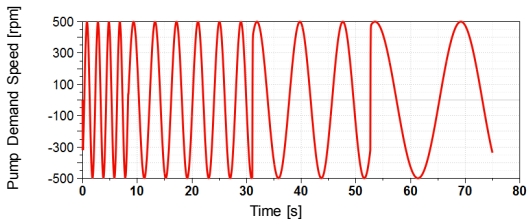

(a) Pump input pattern

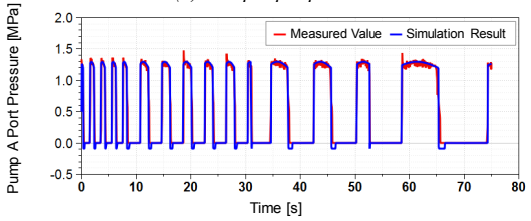

(b) Pressure response at Pump A Port

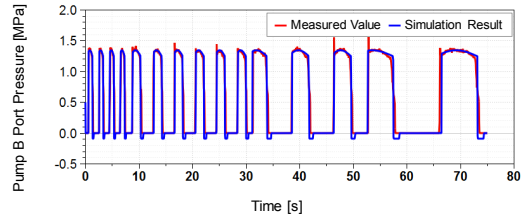

(c) Pressure response at Pump B Port

Figure 7. Result of passive flow compensation valve simulation

TABLE II. COMPENSATION VALVE MODEL PARAMETERS

Ball Diameter D (mm)	10
Rod Diameter d_1 (mm)	3
Seat Diameter d_1 (mm)	5
Stroke L_x (mm)	2
Balls and Rod Weight m (kg)	20
Stiction Force f_{s0} (N)	1.138

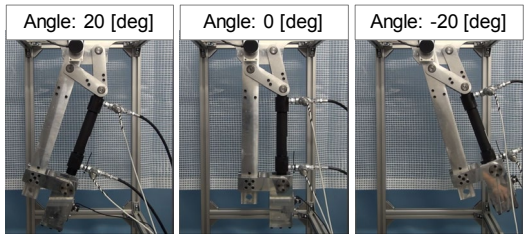

Figure 8. Motion of the bench

Data for validation were measured using the hydraulic circuit shown in Fig. 1. To measure the switching behavior of the passive flow compensation valve, Valves 1a and 1b were completely closed, and the pressure at the ports of Pumps A and B were measured. For the test pattern, the pump rotation speed pattern was given as a sine wave in which the pump discharge flow rate and direction as well as the frequency changed. The parameters in the model were adjusted to match the measured pressure. Fig. 6 illustrates the simulation model of the experimental circuit.

Fig. 7(a) shows the rotational speed pattern of the pump used for validation. The results of the parameter validation are shown in Figs. 7(b) and (c). The red line denotes the result of measurement in the actual circuit, and the blue line denotes the result of the simulation. The pressure responses show that the pressure at the ports of Pumps A and B alternately increase to the relieve pressure as the flow rate of the pump increases and decreases and the direction changes. The timing when the pressure increases or decreases indicates when the poppet opening position changes. By adjusting the parameters of the poppet model, the pressure switching timing of the measured and simulated coincided. This result demonstrates that the poppet model shown in (6) can be used to estimate the internal state. The adjusted parameters are listed in Table II.

C. Evaluation

The position tracking performance was evaluated experimentally for the proposed flow compensation valve control. The newly applied pressure control gain was adjusted to minimize the tracking error for sine waves. Finally, the proposed method was validated by comparing the tracking error for the walking pattern with the case where the proposed system is not applied. The details are presented in Section III.

III. EXPERIMENTS

This section describes the experiments conducted to verify the performance of the proposed flow compensation system.

A. Experimental Setup

Bench test equipment was developed to evaluate the proposed flow compensation system. The hydraulic circuit shown in Fig. 1 is used for the bench. The parameters of hydraulic system are listed in Table I.

A mechanical load device connected to the cylinder was also developed to reproduce the mechanical load during application [14]. The four-bar linkage mechanism was applied to secure a wide-joint driving range for the cylinder. Fig. 8 shows the motion of the bench.

B. Experimental Procedure

The position response to the demand trajectory was analyzed to evaluate the performance of the proposed flow compensation system for the hydraulic direct drive system.

Before implementing the pressure control shown in (11), the unknown parameter V_0 / K is identified. The volume V_0 corresponds to the volume of the hose connecting the pump and valve, as summarized in Table I; thus, it is 9651 mm^3. In addition, because the pressure is low immediately after switching, the operating pressure is a maximum of 2.0 MPa; thus, the bulk modulus K of the mineral oil is 170 to 1600 MPa when air content is a maximum of 0.25% [18]. Therefore, V_0 / K is in the range 56.8–160.9. A sine wave pattern was selected as the operation pattern for the adjustment.

The actual walking pattern was generated using a method we developed for stretched knee walking [1]. The hip joint pitch axis was selected as the subject for the evaluation.

C. Experimental Results

1) Pressure-Based Control Parameter Tuning: Fig. 9 shows the time responses to the sinusoidal position pattern, error, and input pattern of the pump for an amplitude of 20° and frequency of 0.25 Hz. The blue line denotes the results of the previous approach [14], and the red line denotes the result of the proposed system. When the proposed method is not applied, the maximum error is 2.8 degrees.

The unknown parameter of pressure control V_0 / K was experimentally adjusted to minimize the error. The parameter

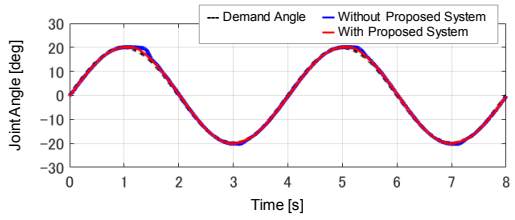

(a) Sinusoidal response

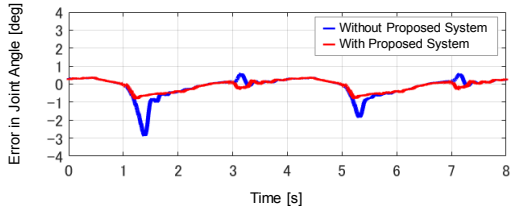

(b) Error

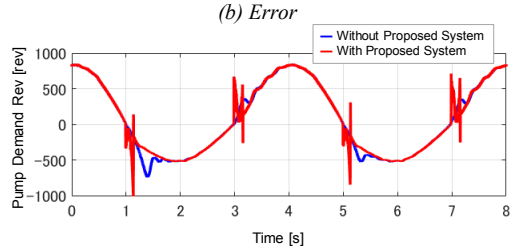

(c) Pump input pattern

Figure 9. Position tracking performance (0.25Hz)

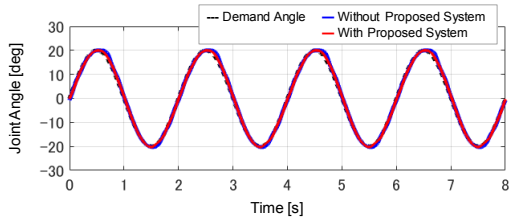

(a) Sinusoidal response

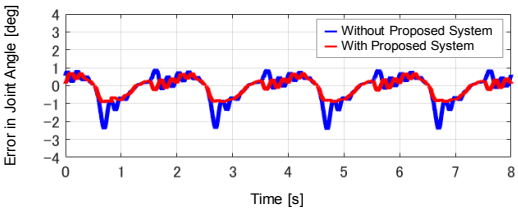

(b) Error

Figure 10. Position tracking performance (0.5Hz)

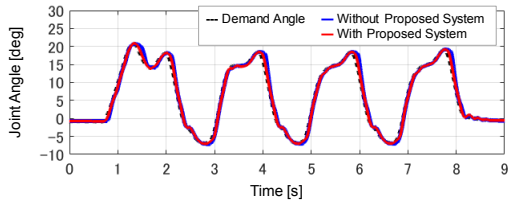

(a) Walking pattern

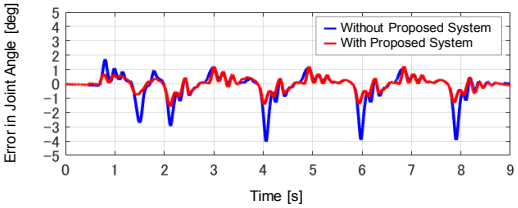

(b) Error

Figure 11. Position tracking performance in walking pattern

value after the adjustment is 86.7. The adjusted value was within the range assumed in advance, and it was confirmed that the proposed design method was effective.

The flow compensation control using the pressure control after the adjustment decreased the error to 0.8 degrees. For conventional flow control, the input value of the pump increased after an error occurred (Fig. 9(c)), whereas in the proposed system, compensation started before an error occurred.

2) Position Tracking Performance: Fig. 10 shows the time responses to the sinusoidal position pattern and the error for an amplitude of 20 degrees and frequency of 0.5 Hz. The blue line denotes the result of the previous approach [14] and the red line denotes the result of the proposed system. When the proposed method was not applied, the maximum error was 2.4 degrees. The application of the proposed method decreased the error to 0.9 degrees. This result demonstrates that the proposed method is effective even if the operating speed of the cylinder changes.

Fig. 11 shows the time responses to the walking pattern and error. The blue line denotes the result of the previous approach [14] and the red line denotes the result of the proposed system. When the proposed method is not applied, the maximum error is 4.1 degrees; when it is applied, the error is reduced to 1.6 degrees. This result demonstrates that a tracking performance superior to the conventional method can be achieved even in the walking pattern.

The actual walking pattern is affected by disturbances such as the reaction force from the ground. Therefore, in future work, it is necessary to investigate the possibility of obtaining robust performance against these disturbances. However, the effect of external force only appears in $P_{cyl\ meter\ in}$ of (10). Therefore, if the pressure can be measured, the proposed approach can be expected to follow the trajectory with high accuracy even when disturbances are experiences during walking. Therefore, by applying this method, more stable walking can be realized.

IV. Conclusion and Future Works

This study developed a flow compensation system for hydraulic direct drive systems. We modeled a passive flow compensation valve for a mounting circuit in which a single rod cylinder and pump were connected in a closed circuit; further, we constructed a model for estimating the internal state. The flow compensation system switched from flow control to pressure control when the valve was switching, depending on the internal state of the passive flow control valve estimated using the proposed model. We adjusted the pressure control parameters to minimize the sine wave pattern error. We demonstrated that the control error in the walking pattern can be reduced from 4.1 to 1.6 degrees by applying the proposed flow compensation system.

In future work, we plan to improve the trajectory tracking performance of the system by compensating for external disturbances, and we plan to study both position and force control. We also plan to build a biped robot that incorporates the planned system and performs walking, hopping, and running.

REFERENCES

[1] Y. Ogura, K. Shimomura, H. Kondo, A. Morishima, T. Okubo, S. Momoki, H. O. Lim, and A. Takanishi, "Human-like walking with knee stretched, heel-contact and toe-off motion by a humanoid robot," *Proc. 2006 IEEE/RSJ Int. Conf. Intell. Robot. Syst.*, pp. 3976–3981, 2006.

[2] T. Otani, K. Hashimoto, S. Hamamoto, S. Miyamae, M. Sakaguchi, Y. Kawakami, H.O. Lim, and A. Takanishi, "Knee joint mechanism that mimics elastic characteristics and bending in human running," *Proc. 2015 IEEE/RSJ Int. Conf. Intell. Robot. Syst.*, pp. 5156–5161, 2015.

[3] J. Urata, Y. Nakanishi, K. Okuda, and M. Inaba, "Design of high torque and high speed leg module for high power humanoid," *Proc. 2010 IEEE/RSJ Int. Conf. Intell. Robot. Syst.*, pp. 4497–4502, 2010.

[4] Y. Ito, S. Nozawa, J. Urata, T. Nkaoka, K. Kobayashi, Y. Nakanishi, K. Okada, and M. Inaba "Development and verification of life-size humanoid with high-output actuation system," *Proc. 2014 IEEE Int. Conf. Robot. Autom.*, pp. 3433–3438, 2014.

[5] I. Park, J. Kim, J. Lee, and J. Oh, "Mechanical design of the humanoid robot platform, HUBO," *Adv. Robot.*, vol. 21, no. 11, pp. 1305–1322, 2007.

[6] Atlas | Boston Dynamics, https://www.bostondynamics.com/atlas, accessed 2019/02/15.

[7] S. Hyon, D. Suewaka, Y. Torii, and N. Oku, ""Design and experimental evaluation of a fast torque-controlled hydraulic humanoid robot," *Trans. Mechatron.*, 2017.

[8] H. Khan, S. Kitano, Y. Goa, D. G. Caldwell, and C. Semini, "Development of the lightweight hydraulic quadruped robot—MiniHyQ," *Proc. IEEE Int. Conf. Technol. Practical Robot Appl.*, pp. 1–6, 2015.

[9] R. Rahmfeld, and M. Ivantysynova, "Energy saving hydraulic actuators for mobile machines." *Proc. 1st Bratislavian Fluid Power Symp.*, pp 47–57, 1998.

[10] J. Zimmerman, E. Busquets, and M. Ivantysynova, "40% fuel savings by displacement control leads to lower working temperatures – a simulation study and measurements," *Proc. 52nd National Conf. Fluid Power*, pp. 693–701, 2011.

[11] H. Kaminaga, S. Otsuki, and Y. Nakamura, "Development of high-power and backdrivable linear electro-hydrostatic actuator," *Proc. 2014 IEEE Int. Conf. Human. Robot.*, pp. 973–978, 2014.

[12] S. Hyon, S. Tanimoto, and S. Asao, "Toward compliant, fast, high-precision, and low-cost manipulator with hydraulic hybrid servo booster," *Proc. 2017 IEEE Int. Conf. Robot. Automat.*, pp. 39–44, 2017.

[13] S. Hyon, and S. Tanimoto, "Joint torque control of a hydraulic manipulator with a hybrid servo booster," *10th JFPS Int. Symp. Fluid Power*, 1C11, 2017.

[14] J. Shimizu, T. Otani, H. Mizukami, K. Hashimoto, and A. Takanishi, "Experimental validation of high-efficiency hydraulic direct-drive system for a biped humanoid robot," *Proc. 2019 IEEE Int. Conf. Robot. Automat.*, pp. 9453–9458, 2019.

[15] J. Shimizu, T. Otani, K. Hashimoto, A. Takanishi, "Downsizing the motors of a biped robot using a hydraulic direct drive system," *Proc. 2018 IEEE-RAS Int. Conf. Human. Robot.*, pp. 580–586, 2018.

[16] J. Shimizu, T. Otani, H. Mizukami, K. Hashimoto, and A. Takanishi, "Experimental validation of hydraulic interlocking drive system for biped humanoid robot," *Proc. 2019 IEEE/RSJ Int. Conf. Intell. Robot. Syst.* (Accepted. Under Publishing).

[17] Takako Industries, INC., http://www.takako-inc.com/, accessed 2019/02/15.

[18] Jitsuyo Yuatsu Pocket Book Editorial Committee, "Jitsuyo Yuatsu Pocket Book" [Practical Hydraulic Pocket Book], Japan Fluid Power Association, pp. 367–368, 2012.